Article

Photonic Crystal Fiber Sensor for Detecting Sulfuric Acid in Different Concentrations

Abdul Mu'iz Maidi [1,*], **Md. Abul Kalam** [2] **and Feroza Begum** [1]

1 Department of Systems Engineering, Faculty of Integrated Technologies, Universiti Brunei Darussalam, Jalan Tungku Link, Gadong, Bandar Seri Begawan BE1410, Brunei
2 School of Civil and Environmental Engineering, Faculty of Engineering and IT, University of Technology Sydney, 15 Ultimo Broadway, Sydney, NSW 2007, Australia
* Correspondence: 21m5101@ubd.edu.bn

Abstract: A high-performance photonic crystal fiber sensor for sulfuric acid detection is designed and investigated, undertaken through a full vector Finite Element Method on COMSOL Multiphysics software to establish the optical properties of effective refractive index, power fraction, relative sensitivity, confinement loss, chromatic dispersion, and propagation constant. Different aqueous sulfuric acid concentrations of 0%, 10%, 20%, 30%, and 40% were selected as the test analytes. The dimensions of two cladding rings of the hexagon- and circular-shaped air holes and a circular core hole denoted outstanding outcomes of relative sensitivity and confinement loss. At 1.1 μm optimum wavelength, 0%, 10%, 20%, 30%, and 40% sulfuric acid concentrations depict relative sensitivities of 97.08%, 97.67%, 98.06%, 98.39%, and 98.67%, respectively, and confinement losses of 1.32×10^{-12} dB/m, 4.11×10^{-12} dB/m, 1.46×10^{-12} dB/m, 6.34×10^{-12} dB/m, and 2.12×10^{-12} dB/m, respectively.

Keywords: photonic crystal fiber; chemical sensor; sulfuric acid; relative sensitivity; confinement loss

1. Introduction

Photonic Crystal Fibers (PCFs) are novel technology of optical fibers featuring a periodic array of air gaps or holes on the axis of the fiber and correspond to its vast recognition in the optics field [1–3]. The structure of the PCF includes the core and cladding, which can be altered with the utilization of countless shapes and designs [4]. In recent years, the flexibility of PCFs has been enthusiastically investigated by researchers to be proposed and implemented in various applications, mainly as sensors [5]. It has been introduced in numerous sensing applications such as gas, temperature, pressure, chemical, and liquid sensors [6–12].

Sulfuric acid is a colorless and odorless aqueous solution with a molar mass of 98.1 g/mol and a density of 1.83 g/cm³. Sulfuric acid is the most adopted chemical employed in the industrial sector for its application in diverse areas of science and technology corresponding to its use in fertilizer production, batteries, mineral dissolution and processing, and manufacturing resins [13,14]. As sulfuric acid has a high density and its nature is to corrode, it must be diluted to specific concentrations to accommodate the desired results [14]. Moreover, this chemical has impacted the climate and environment through acid rain. Thus, a chemical sensor for sulfuric acid detection is needed.

Few researchers have suggested PCFs for chemical sensing, such as a group of researchers [15] who presented an analyte-infiltrated PCF sensor consisting of 9 circular core holes and 36 cladding air holes in three layers, operating within the infrared region (1.0 μm to 1.7 μm). At the optimal wavelength of 1.33 μm, the PCF sensor assessed relative sensitivity of 55.56% and other optical properties of V-Parameter, spot size, beam divergence, and nonlinearity. Podder et al. [16] suggested a PCF sensor design with three rings of cladding and an elaborative array of elliptical holes as the core with sulfuric acid

of different concentrations as the test analyte. The complex core PCF sensor evaluated optical properties of birefringence, power fraction, relative sensitivity, confinement loss, and effective area. At its optimum wavelength and concentration, the chemical sensor assessed relative sensitivity of 62.1% and confinement loss of order 10^{-15} dB/m. Caroline et al. [17] introduced a PCF sensor for sulfuric acid detection, which obtained 68.5% relative sensitivity and estimated 10^{-3} dB/m for confinement loss. The fiber design consists of a complex core design of 16 circular and single rectangular hollow holes to be infiltrated with sulfuric acid and three rings cladding air holes. It also measured results of birefringence and effective area. Another group of researchers [18] proposed a PCF sensor with a suggested structure of three elliptical core holes and three layers of cladding air holes, evaluating performances of relative sensitivity, confinement loss, chromatic dispersion, effective area, and nonlinear coefficient. The hexagonal lattice sensor exhibits confinement loss of order 10^{-10} dB/m and a relative sensitivity of 74.5%, at 1.3 µm operating wavelength. Then, a hexagonal lattice PCF sensor of five cladding rings and a hexagon core hole has been proposed by Eid et al. [19] for chemical sensing exhibiting outstanding results for relative sensitivity of 97.89% and order of 10^{-10} dB/m for confinement loss. Additionally, other optical parameters of numerical aperture and nonlinearity were assessed to analyze its performance.

In the literature [15–19], the researchers have suggested elaborate designs that pose fabrication difficulties. These designs contain numerous core holes and larger layers of cladding air holes, which is susceptible to manufacturing errors. Hence, a simple design is needed to facilitate the ease of fabrication. In this research study, the proposed structure consists of 18 cladding air holes and a single hollow circular core hole to be infiltrated with a sulfuric acid analyte of different concentrations for detection. The design of a photonic crystal fiber chemical sensor is manipulated to assess remarkable results of relative sensitivity, confinement loss, chromatic dispersion, and propagation constant. With the variations in operating wavelength from 0.8 µm to 1.8 µm, the performance of the proposed PCF sensor has been studied carefully. At the optimum wavelength, it deduced relative sensitivity of more than 97% and confinement loss in the order of 10^{-12} dB/m.

2. Design

A simple PCF sensor has been designed and planned for chemical sensing and the schematic cross-sectional diagram that consists of a core, cladding, and Perfectly Matched Layer (PML) is illustrated in Figure 1. For the ease of fabrication, a single circular air hole to be infiltrated is assigned as the core of the fiber with a diameter denoted as *d*. Two layers of air holes are situated along the cladding region to allow confinement of light in the core and achieve low loss of the design. The first layer consists of hexagonal air holes with a corner-to-corner length *l* in a hexagonal lattice, followed by circular air holes with diameter *d* in a similar lattice arrangement. According to the literature [20], hexagonal holes can be manufactured precisely and with fewer defects. The PML is offset on the outer structure of the fiber. Correspondingly, the air filling fraction of the cladding is posed at a high value to acquire an optically dense core than the cladding, which preserves the modified total internal reflection (m-TIR) as the guiding mechanism.

Silica is chosen for the background material of the fiber sensor. The diameter of the core and cladding holes *d* = 2.94 µm, the length of the hexagonal cladding holes *l* = 3.36 µm, and the pitch distance of neighboring air holes Λ = 3.0 µm. The PML is optimized to be 10% of the cladding diameter to meet the boundary condition. The circular core and cladding hole diameter, hexagonal cladding hole length, and pitch distance are defined as the global parameters. To investigate the fabrication toleration, the dimensions of the global parameters are varied by ± 0.1 µm. For the increase of 0.1 µm, the dimensions shall be *d* = 3.04 µm, *l* = 3.46 µm, and Λ = 3.1 µm, while a decrease of 0.1 µm equates to *d* = 2.84 µm, *l* = 3.26 µm, and Λ = 2.9 µm.
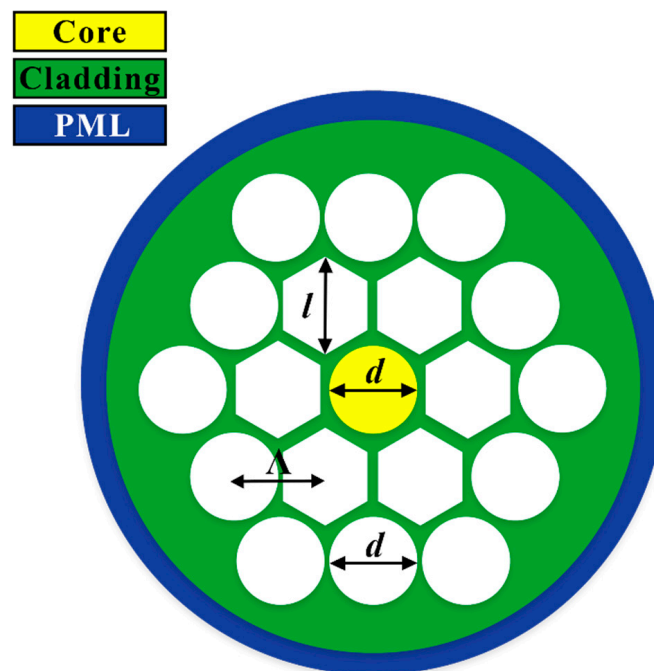
Figure 1. Proposed PCF design for chemical sensing.

The proposed infiltration technique for this fiber design may follow the suggestion in reference [21], where the method to fill liquid in the PCF is by capillarity. One fiber end is dipped into the liquid while the other is left open at room pressure. The condition is the affinity with the PCF material; the cohesive forces between the molecules of the liquid must be lower than the adhesion forces of the liquid with the channel material. However, for selective hole infiltration, this can be achieved by directly blocking one by one the selected holes with some other material such as polymerizable glue. Another method of infiltration is described in reference [22]; the PCF is spliced with a standard single-mode fiber (SMF), where the cores of the PCF and SMF are connected. The connection between the SMF and PCF is called the transition region and functions as a fiber mask. Thus, since the cladding core holes are blocked, liquid can be infiltrated into the core region only, flowing from the SMF into the PCF.

3. Methodology

The simulation process of the proposed PCF has been conducted using COMSOL Multiphysics version 5.5 by implementing a Full Vector Finite Element Method (FV-FEM) for numerical analysis. This simulation method maps small homogeneous triangular segments onto the axes of the PCF, a procedure called meshing. A finer element size meshing has been correctly mapped on the fiber design and has a complete mesh, which consists of 12,324 triangular elements, 1446 edge elements, and 96 vertex elements. For chemical sensing of sulfuric acid, the test analyte is allowed to be infiltrated into the fiber for detection. The refractive indices of sulfuric acid with different concentrations of 0%, 10%, 20%, 30%, and 40% at wavelengths from 0.8 to 1.8 μm is given in Table 1 [16,23,24]. The different concentrations of sulfuric acid are obtained through diluting with water; 0% sulfuric acid and 100% water, 10% sulfuric acid and 90% water, 20% sulfuric acid and 80% water, 30% sulfuric acid and 70% water, and 40% sulfuric acid and 60% water.

The main optical properties numerically investigated for the proposed PCF design are effective refractive index, power fraction, relative sensitivity, confinement loss, chromatic dispersion, and propagation constant. The optical properties are assessed to govern its effectiveness and potential practical use for chemical sensing.

Table 1. Refractive index of sulfuric acid of different concentrations with respect to wavelength [16,23,24].

Wavelength (µm)	Refractive Index of Sulfuric Acid in Different Concentrations				
	0%	10%	20%	30%	40%
0.8	1.3290	1.3451	1.3576	1.3701	1.3821
0.9	1.3280	1.3440	1.3565	1.3690	1.3810
1.0	1.3270	1.3430	1.3555	1.3680	1.3800
1.1	1.3260	1.3420	1.3545	1.3670	1.3790
1.2	1.3245	1.3405	1.3530	1.3655	1.3775
1.3	1.3230	1.3390	1.3515	1.3640	1.3760
1.4	1.3210	1.3370	1.3495	1.3620	1.3740
1.5	1.3190	1.3350	1.3475	1.3600	1.3720
1.6	1.3170	1.3330	1.3455	1.3580	1.3700
1.7	1.3145	1.3305	1.3430	1.3555	1.3675
1.8	1.3120	1.3280	1.3405	1.3530	1.3650

With the selected silica background material and the core hole injected with the test analyte, the effective refractive index n_{eff} can be measured and modelled using the Sellmeier's equation given by [25]:

$$n_{\text{eff}}(\lambda) = \sqrt{1 + \frac{A_1\lambda^2}{\lambda^2 - B_1} + \frac{A_2\lambda^2}{\lambda^2 - B_2} + \frac{A_3\lambda^2}{\lambda^2 - B_3}} \qquad (1)$$

where λ is the operating wavelength, and A_i and B_i (i = 1, 2, and 3) are the Sellmeier coefficients for the specific material.

Power fraction F is the quantification of power flowing through the desired region of the PCF, and it is defined as the ratio of power in a particular region to that of the total fiber. It is expressed by Poynting's theorem as [26–28]:

$$F = \frac{(sample) \int Re\left(E_x H_y - E_y H_x\right)dxdy}{(total) \int Re\left(E_x H_y - E_y H_x\right)dxdy} \times 100 \qquad (2)$$

where, E_x, E_y, and H_x, H_y are the transverse electric and magnetic fields of the guided mode, respectively. The integral in the numerator is integrated over the liquid analyte samples at the core, while the integral in the denominator is integrated over all-fiber regions.

Relative sensitivity S determines the sensing capacity of the PCF sensor to detect analytes by matching the refractive indices and is achieved by measuring the light intensity, which interacts with the analyte. It is defined as [26–28]:

$$S = \frac{n_r}{n_{\text{eff}}} \times F \qquad (3)$$

where n_r is the refractive index of the sensed material and F is the power fraction.

Confinement loss L measures the degree of loss of the waveguide from the core region of the fiber, and is defined as [28–31]:

$$L = \frac{40\pi}{\ln(10)\lambda}\text{Im}[n_{\text{eff}}] \times 10^6 \qquad (4)$$

where $\text{Im}[n_{\text{eff}}]$ is the imaginary part of the effective mode index.

Chromatic dispersion D occurs when a fraction of light power propagating through the cladding region is faster than the core region. It can be quantified by [29,31]:

$$D = -\frac{\lambda}{c}\frac{d^2}{d\lambda^2}\text{Re}[n_{\text{eff}}] \qquad (5)$$

where c is the speed of light and $\text{Re}[n_{\text{eff}}]$ is the real part of the effective refractive index.

Propagation constant *P* of an electromagnetic wave is the measure of alteration by the amplitude of the wave as it propagates in each direction. Therefore, the propagation constant is defined as [32,33]:

$$P = \frac{2\pi n_{\text{eff}}}{\lambda} \tag{6}$$

4. Results and Discussion

The performance of the proposed PCF with different concentrations of sulfuric acid diluted in water has been analyzed by considering the different results of optical properties including power fraction, relative sensitivity, confinement loss, chromatic dispersion, and propagation constant. Figure 2 shows the simulated mode profile of the PCF with the liquid test analyte at a wavelength of 1.1 μm that demonstrates the interaction of light and test analyte and confined within the core of the proposed fiber.
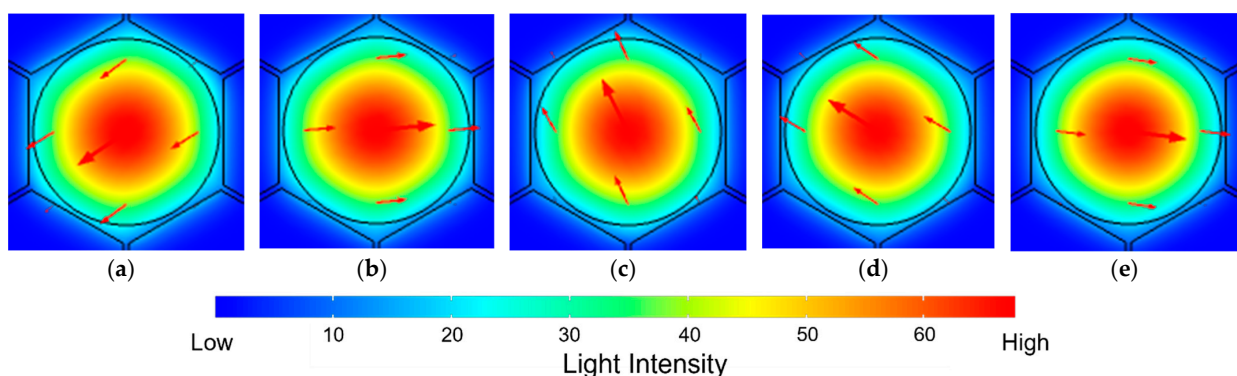

Figure 2. Mode profile of the proposed PCF at 1.1 μm with sulfuric acid concentrations of (**a**) 0% (**b**) 10% (**c**) 20% (**d**) 30% (**e**) 40%.

Figure 3 represents the effective refractive index of the test analytes in relation to the operating wavelength from 0.8 μm to 1.8 μm. It is evident that the effective refractive index decreases with the increase of operating wavelength. This behavior is because the electromagnetic signal at lower wavelengths prefers to propagate through the high refractive index region and as the wavelength increases, it has stronger capabilities to overflow to the cladding region. Furthermore, as the concentration of sulfuric acid increases, the values of the effective index increase.
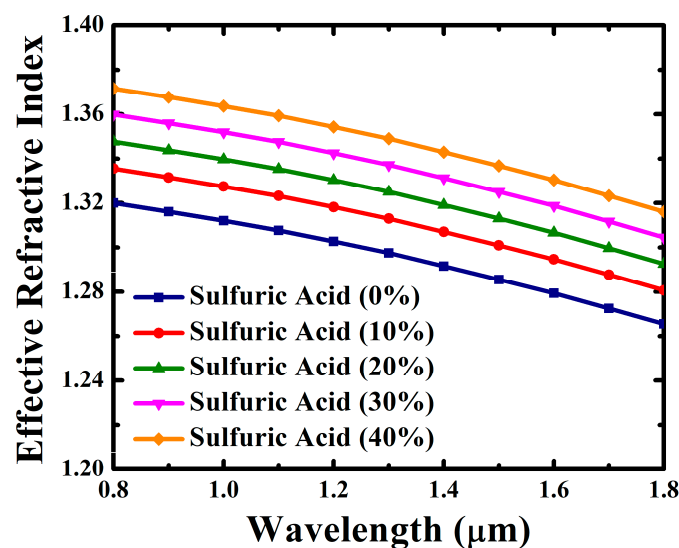

Figure 3. Effective refractive index of the proposed PCF with sulfuric acid of different concentrations: 0%, 10%, 20%, 30%, and 40%.

The relationship between the power fraction of the PCF sensor with respect to wavelength is shown in Figure 4. It can be seen that the power fractions for 20%, 30%, and 40% concentrations of sulfuric acid decrease non-uniformly as the wavelength increases from 0.8 μm to 1.8 μm. However, sulfuric acid analyte concentrations of 0% and 10% increase up to 1.0 μm, before subsequently decreasing as wavelength further increases. The results of power fractions are above 92%, which deduces high power flowing through the core of the fiber sensor.
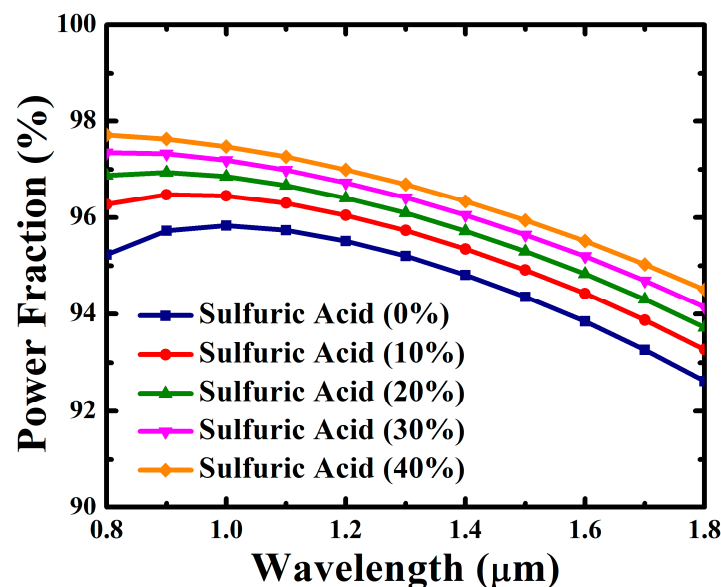

Figure 4. Power fraction of the proposed PCF sensor with 0%, 10%, 20%, 30%, and 40% concentrations of sulfuric acid for different operating wavelengths.

Figure 5 presents the behavior of relative sensitivity with respect to the operating wavelength of sulfuric acid at different concentrations. Relative sensitivities of the PCF sensor rise as wavelength increases from 0.8 μm to 1.1 μm and subsequently decreases as the wavelength increases further. Relative sensitivity is closely related to effective refractive index and power fraction; therefore, a similar trend is noticed between the optical properties. Surrounding the core hole with hexagonal-shaped air holes permits nearly total confinement of light, hence, high interaction of waveguide and test analytes. Thus, tremendously high relative sensitivities have been attained. At 1.1 μm, the optimum values of relative sensitivity are obtained, which are 97.08%, 97.67%, 98.06%, 98.39%, and 98.67% for concentrations of 0%, 10%, 20%, 30%, and 40% of sulfuric acid, respectively. The optimum results are found at a wavelength of 1.1 μm; thus, the other values of optical properties are also obtained at 1.1 μm.

Figure 6 illustrates the assessed results of confinement loss with the variation of operating wavelength between the range 0.8–1.8 μm. It is distinguished that confinement loss increases with the increase of wavelength, a distinct behavior of the waveguide as light tends to escape through the core as wavelength increases. Moreover, applying hexagonal air holes about the core hole reduces the leakage of light into the cladding, hence, low results of confinement losses. A lower confinement loss is observed when a higher concentration of sulfuric acid is filled in the core of the proposed PCF sensor, while higher confinement losses are seen as the percentage concentration of the analyte is decreased. The optimum results of confinement losses of sulfuric acid at concentrations of 0%, 10%, 20%, 30%, and 40% are 1.32×10^{-12} dB/m, 4.11×10^{-12} dB/m, 1.46×10^{-12} dB/m, 6.34×10^{-12} dB/m, and 2.12×10^{-12} dB/m, respectively, at 1.1 μm operating wavelength. With low confinement losses obtained, the PCF design displays potential implementation in optical transmissions, besides sensing applications.
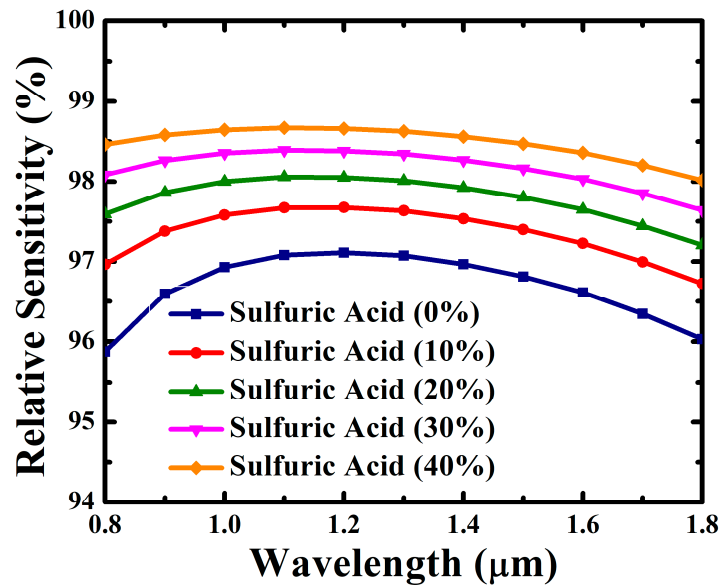
Figure 5. Relative sensitivity of the proposed PCF sensor with 0%, 10%, 20%, 30%, and 40% concentrations of sulfuric acid for different operating wavelengths.
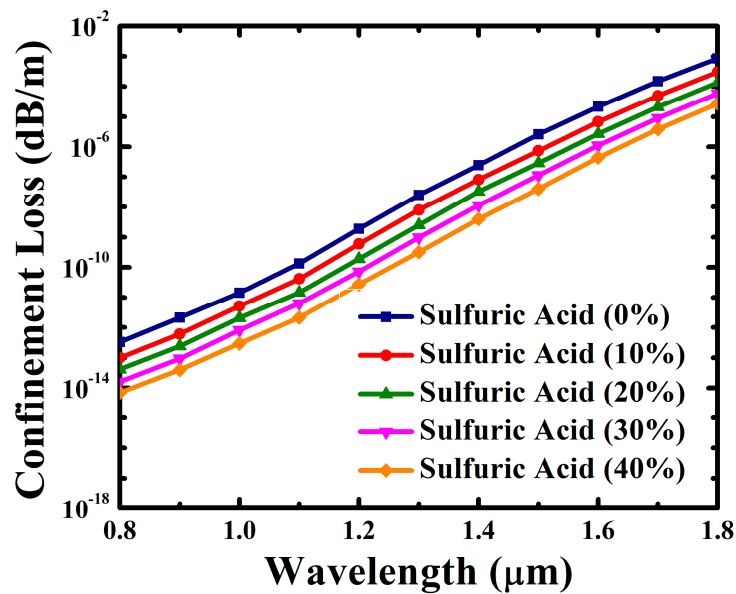

Figure 6. Confinement loss of the proposed PCF sensor with 0%, 10%, 20%, 30%, and 40% concentrations of sulfuric acid for different operating wavelengths.

Chromatic dispersion results of the proposed PCF with respect to operating wavelength for the different sulfuric acid concentrations (0%, 10%, 20%, 30%, and 40%) are illustrated in Figure 7. It is observed from the graph that chromatic dispersion decreases as wavelength increases within the wavelength range of 0.8–1.8 μm. For the different concentrations, it has an ultra-flattened chromatic dispersion as the variation change from 0.8 μm to 1.8 μm is small. The chromatic dispersions assessed at 1.1 μm are −0.0051 ps/nm.km, −0.0052 ps/nm.km, −0.0053 ps/nm.km, −0.0054 ps/nm.km, and −0.0055 ps/nm.km for percentage concentration of 0%, 10%, 20%, 30%, and 40%, respectively. With such low chromatic dispersions, the PCF structure can also be used in optical communications.

The propagation constant results with respect to the wavelength of the different concentrations of sulfuric acid are represented in Figure 8. For the concentrations of 0%, 10%, 20%, 30%, and 40%, propagation constant decreases with the wavelength increase from 0.8 μm to 1.8 μm. The propagation constant is linearly relative to the effective

refractive index for the slight variation of the operating wavelength. Hence, with increasing wavelength, the propagation reduces with the function of effective refractive index and the propagation constant decreases non-uniformly. At operating wavelength of 1.1 μm, the propagation constants for sulfuric concentration of 0% is 7.47×10^6 rad/m, 10% is 7.56×10^6 rad/m, 20% is 7.63×10^6 rad/m, 30% is 7.70×10^6 rad/m, and 40% is 7.76×10^6 rad/m.
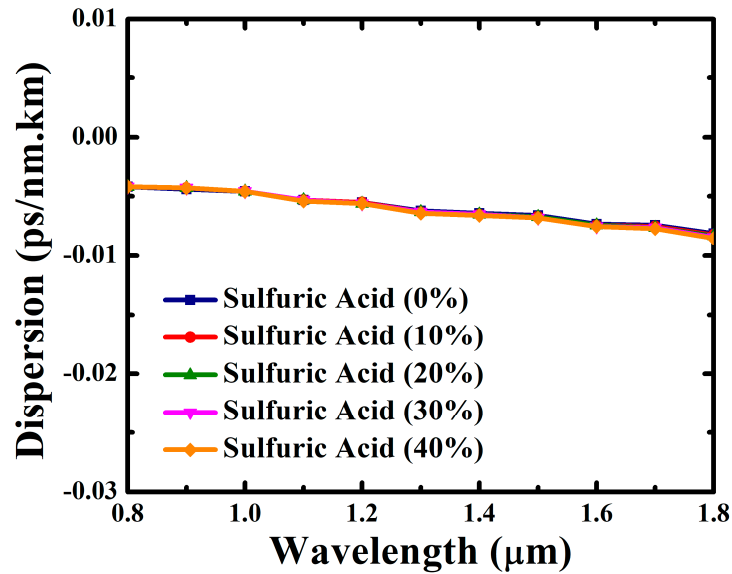

Figure 7. Chromatic dispersion of the proposed PCF sensor with 0%, 10%, 20%, 30%, and 40% concentrations of sulfuric acid for different operating wavelengths.
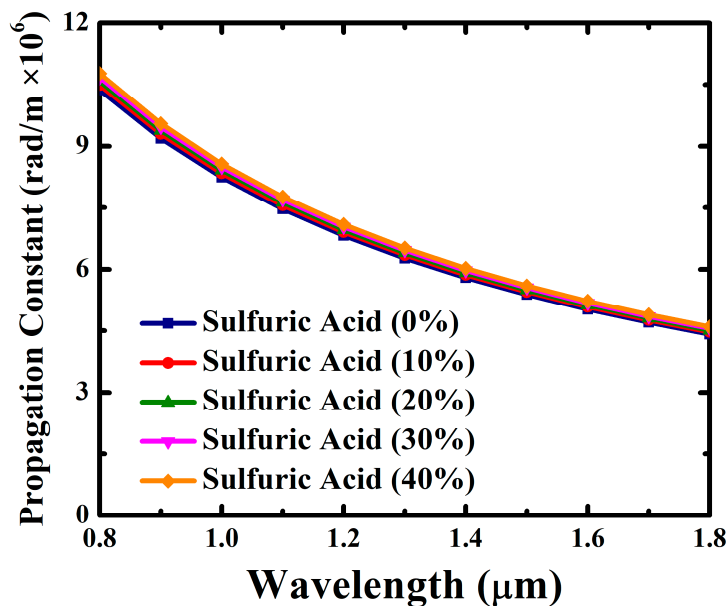

Figure 8. Propagation constant of the proposed PCF sensor with 0%, 10%, 20%, 30%, and 40% concentrations of sulfuric acid for different operating wavelengths.

In addition, to overview the performance of the proposed PCF sensor with the change in concentration of the analyte, the results of relative sensitivity and confinement loss at different concentrations of sulfuric acid for 0%, 10%, 20%, 30%, and 40% is shown in Figure 9. It can be observed that the relative sensitivities of the proposed PCF increase as the percentage concentration of sulfuric acid increases. At the same time, the results of confinement losses decrease with the increases in sulfuric acid concentration from 0%

to 40%. This effect is due to the increase in the refractive index of the analyte when the concentration of sulfuric acid increases, which raises the interaction between the light and test analyte.
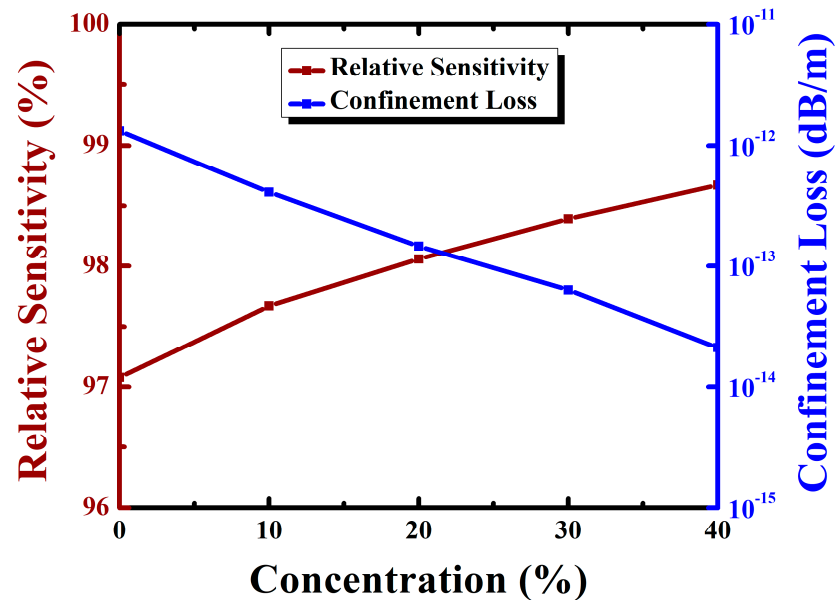

Figure 9. Variation of relative sensitivity and confinement loss with respect to concentrations of sulfuric acid (0%, 10%, 20%, 30%, and 40%).

An investigation of the variation of the dimensions of the global parameters to relative sensitivity is performed to outline the fabrication tolerance and sensing performance of the proposed sensor. The global dimensions are varied by ±0.1 μm and shown in the Table 2. Even with small modifications in the air hole diameter and pitch distance, the relative sensitivity does not deviate from the optimum value, as seen from the table. Thus, this demonstrates the durability of the proposed design.

Table 2. Performance analysis against the variation of global dimension at $\lambda = 1.1$ μm.

Change in Dimension	Relative Sensitivity (%)				
	0% H_2SO_4	10% H_2SO_4	20% H_2SO_4	30% H_2SO_4	40% H_2SO_4
+0.1 μm	97.04	97.65	98.04	98.38	98.66
Optimum	97.08	97.67	98.06	98.39	98.67
−0.1 μm	97.11	97.69	98.07	98.40	98.68

Furthermore, a comparison between the proposed fiber and prior PCFs is presented in Table 3. It can be observed from the table below that the proposed PCF establishes the highest relative sensitivity and lowest confinement loss.

Table 3. Comparison of performance among prior PCFs and proposed PCF at $\lambda = 1.1$ μm.

	Relative Sensitivity (%)	Confinement Loss (dB/m)
Ref. [15]	54.2	-
Ref. [16]	62.1	$\sim 10^{-15}$
Ref. [17]	68.5	$\sim 10^{-3}$
Ref. [18]	79.2	$\sim 10^{-10}$
Ref. [19]	97.5	$\sim 10^{-9}$
Proposed PCF	98.7	$\sim 10^{-13}$

5. Conclusions

Sulfuric acid is a substance that benefited the industrial sector in its diversified usage but through restricted concentrations due to its corrosive nature. Therefore, a chemical PCF sensor has been proposed for sensing sulfuric acid of different concentrations. A simple sensor structure of two claddings ring of circular and hexagonal holes and a circular core has been introduced that has been numerically analyzed by a full vector FEM simulation technique. The ideal results are obtained at 1.1 μm, which depicts high sensitivities of 97.08% for 0% concentration, 97.67% for 10% concentration, 98.06% for 20% concentration, 98.39% for 30% concentration, and 98.67% for 40% concentration, and low confinement losses of 1.32×10^{-12} dB/m, 4.11×10^{-12} dB/m, 1.46×10^{-12} dB/m, 6.34×10^{-12} dB/m, and 2.12×10^{-12} dB/m for 0%, 10%, 20%, 30%, and 40% concentrations of sulfuric acid, respectively. The results obtained above highlighted that the proposed fiber has the competency for sensing chemicals of varying concentrations and compliments its suitability in optical communication and other sensing applications.

Author Contributions: Conceptualization, A.M.M. and F.B.; methodology, A.M.M. and F.B.; software, A.M.M. and F.B.; validation, M.A.K. and F.B.; formal analysis, A.M.M. and F.B.; investigation, A.M.M. and F.B.; resources, F.B.; data curation, A.M.M. and F.B.; writing—original draft preparation, A.M.M.; writing—review and editing, M.A.K. and F.B.; visualization, F.B.; supervision, F.B.; project administration, F.B.; funding acquisition, F.B. All authors have read and agreed to the published version of the manuscript.

Institutional Review Board Statement: Not applicable.

Informed Consent Statement: Not applicable.

Data Availability Statement: Not applicable.

Conflicts of Interest: The authors declare no conflict of interest.

References

1. Hansen, T.P.; Broeng, J.; Libori, S.E.B.; Knudsen, E.; Bjarklev, A.; Jensen, J.R.; Simonsen, H. Highly birefringent index-guiding photonic crystal fibers. *IEEE Photonics Technol. Lett.* **2001**, *13*, 588–590. [CrossRef]
2. Reeves, W.; Knight, J.; Russell, P.; Roberts, P. Demonstration of ultra-flattened dispersion in photonic crystal fibers. *Opt. Express* **2002**, *10*, 609. [CrossRef]
3. Habib, M.A.; Anower, M.S.; Hasan, M.R. Ultrahigh birefringence and extremely low loss slotted-core microstructure fiber in terahertz regime. *Curr. Opt. Photonics* **2017**, *1*, 567–572. [CrossRef]
4. Pinto, A.M.R.; Lopez-Amo, M. Photonic crystal fibers for sensing applications. *J. Sens.* **2012**, *2012*, 598178. [CrossRef]
5. Troia, B.; Paolicelli, A.; De, F.; Passaro, V.M.N. Photonic Crystals for Optical Sensing: A Review. In *Advances in Photonic Crystals*; IntechOpen: Rijeka, Croatia, 2013. [CrossRef]
6. Gahir, H.K.; Khanna, D. Design and development of a temperature-compensated fiber optic polarimetric pressure sensor based on photonic crystal fiber at 1550 nm. *Appl. Opt.* **2007**, *46*, 1184–1189. [CrossRef]
7. Rifat, A.A.; Ahmed, K.; Asaduzzaman, S.; Paul, B.K.; Ahmed, R. Development of photonic crystal fiber-based gas/chemical sensors. In *Computational Photonic Sensors*; Springer: Cham, Switzerland, 2018. [CrossRef]
8. Martynkien, T.; Szpulak, M.; Urbanczyk, W. Modeling and measurement of temperature sensitivity in birefringent photonic crystal holey fibers. *Appl. Opt.* **2005**, *44*, 7780–7788. [CrossRef]
9. Bock, W.J.; Jiahua, C.; Eftimov, T.; Urbanczyk, W. A photonic crystal fiber sensor for pressure measurements. In Proceedings of the IMTC 2005—Instrumentation and Measurement Technology Conference, Ottawa, ON, Canada, 17–19 May 2005; Volume 2, pp. 1177–1181. [CrossRef]
10. Asaduzzaman, S.; Ahmed, K. Proposal of a gas sensor with high sensitivity, birefringence and nonlinearity for air pollution monitoring. *Sens. Bio-Sens. Res.* **2016**, *10*, 20–26. [CrossRef]
11. Asaduzzaman, S.; Ahmed, K.; Bhuiyan, T.; Farah, T. Hybrid photonic crystal fiber in chemical sensing. *Springerplus* **2016**, *5*, 748. [CrossRef]
12. Leon, M.J.B.M.; Kabir, M.A. Design of a liquid sensing photonic crystal fiber with high sensitivity, bireferingence & low confinement loss. *Sens. Bio-Sens. Res.* **2020**, *28*, 100335. [CrossRef]
13. Niger, M.; Hasin, T.F.; Nizami, M.A.F.; Rafee, M.A. Three Modified Structures of Photonic Crystal Fiber for Estimation of Sulfuric Acid Concentration with Low Confinement Loss and Negative Dispersion. In Proceedings of the 2019 4th International Conference on Electrical Information and Communication Technology (EICT 2019), Baku, Azerbaijan, 20–22 December 2019. [CrossRef]

14. Fraenkel, D. Structure and ionization of sulfuric acid in water. *New J. Chem.* **2015**, *39*, 5124–5136. [CrossRef]
15. Islam, S.; Kumar, B.; Ahmed, K. Liquid-infiltrated photonic crystal fiber for sensing purpose: Design and analysis. *Alex. Eng. J.* **2018**, *57*, 1459–1466. [CrossRef]
16. Podder, E.; Hossain, M.B.; Jibon, R.H.; Bulbul, A.A.M.; Mondal, H.S. Chemical sensing through photonic crystal fiber: Sulfuric acid detection. *Front. Optoelectron.* **2019**, *12*, 372–381. [CrossRef]
17. Caroline, B.E.; Umamaheswari, P.; Jayasri, R.; Kumar, D.S. Investigation on the detection of sulfuric acid using photonic crystal fiber sensor. In Proceedings of the 2020 7th International Conference on Smart Structures and Systems (ICSSS 2020), Chennai, India, 21–24 July 2020. [CrossRef]
18. Maidi, A.M.; Yakasai, I.; Abas, P.E.; Nauman, M.M.; Apong, R.A.; Kaijage, S.; Begum, F. Design and Simulation of Photonic Crystal Fiber for Liquid Sensing. *Photonics* **2021**, *8*, 16. [CrossRef]
19. Eid, M.M.A.; Habib, A.; Anower, S.; Nabih, A.; Rashed, Z. Highly sensitive nonlinear photonic crystal fiber based sensor for chemical sensing applications Highly sensitive nonlinear photonic crystal fiber based sensor for chemical sensing applications. *Microsyst. Technol.* **2020**, *27*, 1007–1014. [CrossRef]
20. Amouzad Mahdiraji, G.; Chow, D.M.; Sandoghchi, S.R.; Amirkhan, F.; Dermosesian, E.; Yeo, K.S.; Kakaei, Z.; Ghomeishi, M.; Poh, S.Y.; Yu Gang, S.; et al. Challenges and Solutions in Fabrication of Silica-Based Photonic Crystal Fibers: An Experimental Study. *Fiber Integr. Opt.* **2014**, *33*, 85–104. [CrossRef]
21. Algorri, J.; Zografopoulos, D.; Tapetado, A.; Poudereux, D.; Sánchez-Pena, J. Infiltrated Photonic Crystal Fibers for Sensing Applications. *Sensors* **2018**, *18*, 4263. [CrossRef]
22. Zhang, B.M.; Lai, Y.; Yuan, W.; Seah, Y.P.; Shum, P.P.; Yu, X.; Wei, H. Laser-assisted lateral optical fiber processing for selective infiltration. *Opt. Express* **2014**, *22*, 2675. [CrossRef]
23. Hale, G.M.; Querry, M.R. Optical Constants of Water in the 200-nm to 200-μm Wavelength Region. *Appl. Opt.* **1973**, *12*, 555. [CrossRef]
24. Krieger, U.K.; Mössinger, J.C.; Luo, B.; Weers, U.; Peter, T. Measurement of the refractive indices of H_2SO_4–HNO_3–H_2O solutions to stratospheric temperatures. *Appl. Opt.* **2000**, *39*, 3691. [CrossRef]
25. Akowuah, E.K.; Gorman, T.; Ademgil, H.; Haxha, S.; Robinson, G.K.; Oliver, J.V. Numerical Analysis of a Photonic Crystal Fiber for Biosensing Applications. *IEEE J. Quantum Electron.* **2012**, *48*, 1403–1410. [CrossRef]
26. Yakasai, I.; Abas, P.E.; Kaijage, S.F.; Caesarendra, W.; Begum, F. Proposal for a quad-elliptical photonic crystal fiber for terahertz wave guidance and sensing chemical warfare liquids. *Photonics* **2019**, *6*, 78. [CrossRef]
27. Yakasai, I.K.; Abas, P.E.; Ali, S.; Begum, F. Modelling and simulation of a porous core photonic crystal fibre for terahertz wave propagation. *Opt. Quantum Electron.* **2019**, *51*, 122. [CrossRef]
28. Maidi, A.M.; Abas, P.E.; Petra, P.I.; Kaijage, S.; Zou, N.; Begum, F. Theoretical Considerations of Photonic Crystal Fiber with All Uniform-Sized Air Holes for Liquid Sensing. *Photonics* **2021**, *8*, 249. [CrossRef]
29. Begum, F.; Namihira, Y.; Razzak, S.M.A.; Kaijage, S.F.; Hai, N.H.; Miyagi, K.; Higa, H.; Zou, N. Flattened chromatic dispersion in square photonic crystal fibers with low confinement losses. *Opt. Rev.* **2009**, *16*, 54–58. [CrossRef]
30. Begum, F.; Namihira, Y.; Kinjo, T.; Kaijage, S. Supercontinuum generation in photonic crystal fibres at 1.06, 1.31, and 1.55 μm wavelengths. *Electron. Lett.* **2010**, *46*, 1518. [CrossRef]
31. Begum, F.; Abas, P.E. Near infrared supercontinuum generation in silica based photonic crystal fiber. *Prog. Electromagn. Res. C* **2019**, *89*, 149–159. [CrossRef]
32. Priya, K.R.; Raja, A.S.; Sundar, D.S. Design of a dual-core liquid-filled photonic crystal fiber coupler and analysis of its optical characteristics. *J. Opt. Technol.* **2016**, *83*, 569. [CrossRef]
33. Hossain, M.M.; Hossain, M.B.; Amin, M.Z. Small coupling length with a low confinement loss dual-core liquid infiltrated photonic crystal fiber coupler. *OSA Contin.* **2018**, *1*, 953. [CrossRef]